Influence of anodizing surface treatment on the aging behavior in salt-fog environment of aluminum alloy 5083 to fiber reinforced composite adhesive joints

F. Di Franco, V. Fiore*, R. Miranda, D. Badagliacco, M. Santamaria, A. Valenza

Department of Engineering, University of Palermo, Viale delle Scienze, Ed. 6, 90128 Palermo, Italy

Email: vincenzo.fiore@unipa.it

*Corresponding Author

Influence of anodizing surface treatment on the aging behavior in salt-fog environment of aluminum alloy 5083 to fiber reinforced composite adhesive joints

The present work aims to evaluate how an innovative and eco-friendly anodizing process with tartaric-sulfuric acid (TSA) bath and a pore widening in an aqueous solution of NaOH 0.1 M can improve the durability in marine environment of co-cured adhesive joints between an aluminum alloy (AA 5083) and fiber (i.e., glass or basalt) reinforced composite substrates. The aging was carried out by exposing samples to salt-fog spray conditions (5 wt.% NaCl) for 30, 60 and 90 days in a climate chamber, in accordance with ASTM B117. In order to get further insights on the aging behaviour of bonded joints, neat matrix was also exposed to the same environment for 60 days. Quasi-static mechanical tests and morphological analysis through SEM microscope coupled with EDX analyser were carried out to deeper understand how the fracture surfaces change during aging and how this affected the mechanical performances of joints.

Keywords: Adhesive Joint, surface treatment, salt-fog aging, anodizing, basalt, Double Strap Joint

1. Introduction

Nowadays, the usage of composite materials has considerably increased in nautical industry due to their low weight and high mechanical performances [1–3]. These features, indeed, allow to increase cargo or save fuel, thus leading to a reduction of CO_2 emissions. However, two of the critical issues of these materials are related to the high emissions during their production and their no recyclability. A possible solution to these problems consists in the usage of natural fibres as reinforcement of bio-based recyclable epoxy matrix. Natural fibres have found many applications in industry sectors such as nautical or automotive, due to their specific properties such as sustainability, good specific properties, wide availability, and low price. Furthermore, they are renewable and have a low environmental impact [4,5].

Among natural fibres, basalt is considered one of the main candidates for replacing synthetic fibres such as E-glass as reinforcement of composite materials useful for nautical applications. It is a mineral fibre which can be obtained by melting basalt rock from volcano activities. In more detail, its production process does not require the use of any chemical additives such as solvents, pigments, or other hazardous materials. In fact, a continuous filament of basalt fibres can be prepared in a one-step process, consisting of melting and direct extrusion. This material possesses comparable mechanical properties as well as higher thermal stability and chemical inertia in comparison to E-glass (i.e., the most used reinforcement in this field) [6–8]. Other important features of basalt fibre lie in its resistance to corrosion in addition to a very low moisture absorption tendency.

As concerning the matrix phase, it is widely known that the use of synthetic thermosetting polymers should be nowadays reduced due to their difficult disposal at the end of life. In fact, these materials are formed either through polymerization of monomers or by creating chemical crosslinks between linear or branched polymers (i.e., curing process). These irreversible chemical reactions create a cross-linked network of interconnected molecules which cannot be thermally processed further [9]. In this context, several chemical recycling methods based on the use of solvent mixtures have been carried out in the past [10–12]. An alternative sustainable solution consists in the use as curing agent

of cleavable amines that allow to obtain epoxy thermoset matrix which can be recycled yielding thermoplastics, as shown by Cicala et al. [13–16]. They produced fibre reinforced composites, which resulted recyclable by soaking them in mild acetic acid aqueous solutions. Furthermore, the Life Cycle Assessment (LCA) of these materials was assessed showing that recycling and reusing the reinforcing fibres with very little chemical damage are the most important aspects in terms of environmental and economic savings.

When some parts of the ship are difficult to create by using composite materials, it's needed to joint them to traditional materials such as metals, for example by building a superstructure in glass fibre reinforced polymer (GFRP) on metallic hull [17]. Hence, the implementation of composite materials in conjunction with metals into hybrid structural systems is currently developed in several industrial field such as nautical one [18].

In this context, composites and metals can be joined mechanically [19,20], adhesively [18,21] or through a combination of both techniques [22,23]. Among these kind of connections, the adhesive one offers various advantages such as no presence of damage caused by drilling, prevention of degradation phenomena as consequence of galvanic corrosion, high absorption of energy as well as cost and weight reductions due to the absence of a third linking elements [24–26] . Despite this, the interaction between adhesive and substrates often represents the weakness of joined structures. Hence, it is necessary to employ an appropriate surface treatment to overcome this issue.

A wide available literature can be found about several surface treatments such as mechanical abrasion, chemical etching, laser texturing or electrochemical treatments like anodizing process [27–29]. In particular, the latter is able to create an oxide porous layer that could be heightened on the metal surface, thus generating a good interlocking with the adhesive layer and, at the same time, furnishing a corrosion protection to the metal substrate [30–34]. Due to these reasons, this treatment was already used to improve the aging resistance against various environmental condition of metal to metal or metal to composite adhesive joints [35–38]. For example, Golaz et al. [39] evaluated the strength and Griffith's critical strain energy release rate G_{IC} of adhesive joints before and along 13 weeks of

accelerated aging in salted and deionized water at 50 °C, at varying the surface treatments on titanium alloy grade 5. In particular, sandblasting, chemical etching and anodizing treatments were carried out. The experimental results show that the aging decreased the strength and the critical strain energy release rate of bonded joints by 30–70% and that samples anodized had faster mechanical performance decrease. It is worth noting that industrial baths widely used (i.e., phosphoric acid, chromic acid, and sulfuric acid solutions) are toxic (i.e., Cr VI is carcinogenic for human) or do not guarantee a proper corrosion protection. Consequently, the research is nowadays focusing on the use of more eco-friendly baths which also offer a good protection from corrosive environments. Abrahami et al. [40] studied the influence of surface chemistry on the adhesion of epoxy matrix on aluminum alloy 2024-T3 anodized with eco-friendly bath (i.e., PAA, SAA, PSA). XPS analysis on the surface and floating roller peel test in dry and wet conditions were carried out. Results showed that all anodizing technique have a good mechanical resistance in dry condition, while in wet condition the resistance depends on the quantities of OH^- on the surfaces.

Zhang et al. [41] evaluated phosphoric/boric/sulfuric acids anodizing as replacement of chromic acid anodizing. FE-SEM and AFM analyses were carried out to evaluate microstructure and topography of the pre-treated surface, while mechanical tests such as lap shear and wedge to evaluate the adhesion between metal to metal with epoxy adhesive. The results showed how this innovative treatment could improve both bonding strength and corrosion resistance under humid and hot environments.

In this regard, the present paper aims to evaluate for the first time the effect of an innovative and eco-friendly electrochemical process (i.e., Tartaric-Sulfuric acid anodizing) on the aging resistance against salt-fog environmental condition of metal to composite bonded joints. To this scope, treated and untreated (or reference) joints were exposed to salt spray fog (5 wt.% NaCl) at 35° C in a climatic chamber for three months (i.e., 90 days).

2. Experimental

2.1. Materials

The metallic substrate of joints corresponds to Aluminum alloy sheet 5083 series, with nominal thickness 3 mm, length 110 mm, width 160 mm, Young's modulus of elasticity 70 GPa and tensile yield strength 125 MPa.

With the aim of comparing the aging resistance of bonded joints at varying the reinforcement of the composite substrates, two plain weave woven fabrics were used: i.e., glass (with areal weight 200 g/m^2) and basalt fabrics (220 g/m^2), supplied by Hexcel® and Basaltex®, respectively.

The polymeric matrix was obtained by mixing a bio-based epoxy monomer SuperSap® 300 with a cure inhibitor INH (both furnished by Entropy Resins) and an amine curing agent Recyclamine® 301 (furnished by Connora Technologies) with the weight mix ratio 100:32:11 (resin: curing agent: INH). SuperSap® 300 is composed of epoxidized pine oils, bisphenol A/F type resin, benzyl alcohol, and proprietary reactive epoxy diluent. Recyclamine® 301 is a cleavable polyamine ether. The INH inhibitor is added to the mix as a viscosity and pot life modifier. In particular, the pot life extends while the viscosity of the mix lowers by increasing the INH content. The mix ratio was suggested by the supplier datasheet, that also reports the pot life and viscosity equal to 48 min and 500 cPs, respectively.

Following the same procedure described in our previous paper [31] both fabrics (i.e., glass and basalt) were treated with an amino-silane coupling agent (i.e., Sigma-Aldrich (3-Aminopropyl)trimethoxysilane) in order to strengthen the fibre-matrix adhesion in composite substrates.

2.2. Metal surface treatments

In this paper two metallic surface treatments were compared in order to evaluate their effects on the aging behaviour of metal to composite bonded joints: i.e., namely mechanical abrasion and anodizing.

Mechanical abrasion was chosen as reference treatment. In particular, the aluminum substrates were mechanically treated for 20 minutes through an orbital sander Bosch PSS 250 AE with a sandpaper P80 using a number of oscillations of 20000 osc. /min. After that, aluminum substrates were first cleaned in deionized water for 2 minutes and then in an ultrasonic acetone bath for further 5 minutes. All steps were performed at room temperature (i.e., 24 ± 1 °C).

The anodizing treatment was carried out following a multi-step process. Firstly, the metallic substrates were smoothed with the same orbital sander of mechanical treatment and the same number of oscillations, but with sandpaper up to grid 2000. Secondly, they were cleaned in deionized water, after in an ultrasonic bath with acetone for 5 minutes, and then rinsed in deionized water. Thirdly, they were soaked in a 10 wt.% of NaOH aqueous solution at 60°C for 30 s and subsequently rinsed in deionized water. Finally, the samples were immersed in 30% v/v HNO_3 aqueous solution at room temperature for 15 s and then cleaned with deionized water. All reagents were supplied by Sigma-Aldrich. Finally, the anodizing treatment was realized in a bath composed by 0.48 M sulfuric acid and 80 g/l of tartaric acid and water (TSA) [42]. The process parameters were a voltage of 14V at 37 °C for 20 min during a moderate stirring. After these steps, the metallic samples were immersed in a 0.1 M NaOH solution at room temperature for 2 min to widen pores of the oxide layer (Figure 1).

After each treatment (i.e., mechanical abrasion or anodizing), the metallic substrates were dried at room temperature for 24 h before manufacturing of joints.

All samples are codified by using a prefix “REF” and “ANOD” depending on the treatment carried out on the metallic surface (i.e., mechanical abrasion or anodizing) followed by a suffix “GFRP” and “BFRP” as function of the kind of fiber (i.e., glass or basalt) used as reinforcement of the composite substrates (see Table 1). For instance, “REF-GFRP” indicates joints having the metal substrates mechanically abraded and the composite substrates reinforced with glass fabrics.

2.3. Manufacturing of joints and neat matrix samples

Double strap adhesive co-cured joints (160 mm width, 220 mm length) were manufactured through vacuum infusion process by placing two aluminum sheets (110 mm x 160 mm x 3 mm) side by side in a plain mold. In correspondence of the bonded area six dry fabrics (50 mm x 160 mm) of basalt or glass fibers were manually laid up above and below the metal sheets, respectively. Afterwards, a vacuum bag closed the mold and the air inside was pulled out by a two-stage vacuum pump model VE 235 D by Eurovacuum. The dry lay-up contained in the mould was then impregnated by the epoxy matrix, which flows through mainly driven by vacuum.

Before the infusion, the matrix mix was prepared as follow. First, 100 g of epoxy resin was added in a Becher at room temperature, followed by 32 g of curing agent and 11 g of INH. The mix was then slowly stirred manually for 5 minute and degassed for further 2 minutes in a vacuum chamber.

Following this procedure, prismatic samples of neat matrix (80 mm length, 50 mm width, and 5 mm) were also manufactured by pouring the matrix mix in a silicone mold. All joints and neat matrix samples were cured at room temperature (i.e., 24 °C ± 1 °C) for 24 h and then post-cured at 100 °C for further 3 h.

2.4. Salt-fog exposition

The aging behaviour of the co-cured joints was evaluated by exposing them to salt-fog spray condition (5 wt.% NaCl, 35 °C ± 1 °C) in a climate chamber model SC/KWT 450 by WEISS, according to ASTM B 117 standard. At each investigated aging time (i.e., 30, 60 and 90 days), one joint was taken out from the climatic chamber and cut by means of a rotating blade (i.e., Bosch GCM 800 SJ). By doing so, five samples with 25 mm width (Figure 2) were obtained for each manufactured joint as well as for each aging condition, in order to perform the quasi-static tensile tests. For the sake of comparison, five samples from each unaged joint were also tested.

In order to get further insights on the aging behaviour of bonded joints, samples of neat epoxy matrix were also exposed to the same hostile environmental conditions (i.e., salt-fog spray) for three months

(i.e., 90 days). In particular, five prismatic samples (80 mm x 10 mm x 5 mm) were removed from the climatic chamber after 30, 60, and 90 days and mechanically tested under three-point bending configuration. Unaged samples were tested for comparison purpose.

Moreover, the water gain W experienced by the neat matrix during salt-fog exposition was evaluated through the following equation:

$$W = \frac{W_t - W_0}{W_0} 100 \quad (1)$$

where W_0 and W_t are the initial weight and the weight at aging time t, respectively.

2.5. Quasi-static mechanical tests

The tensile characterization of the joints was carried out according to ASTM D 3528 standard. Five samples for each aging condition were tested through a U.T.M. model ETM-C by WANCE, equipped with a 50 kN load cell. The crosshead speed was set equal to 1.27 mm/min. The displacement was measured with a YYU-10/50 extensometer by WANCE, with a gauge length of 50 mm and a full-scale value equal to 20% coupled to the testing machine. The value of the joint strength (or failing stress) was calculated as described in the ASTM standard, i.e., maximum load per total shear area.

Quasi-static three-point bending tests were performed on five neat matrix samples for each aging condition, according to ASTM D 790 standard. To this scope, a U.T.M. model Z005 by Zwick-Roell, equipped with 5 kN load cell. The support span and crosshead speed were set equal to 60 mm and 1.4 mm/min, respectively.

2.6. Analysis of the failure zones

The aluminum alloy surfaces of fractured joints were observed by using a scanning electron microscope model XL30 ESEM by Philips, coupled with EDX. SEM images and EDX information are helpful to evaluate the presence of corrosion products as well as to investigate the morphologies of the metal surfaces after the exposition of the joints to salt-fog environment.

3. Results and discussion

3.1. Quasi-static mechanical tests

The average values and the related standard deviations of maximum strength for compared joints (i.e., REF and ANOD batches) at each aging condition time (i.e., 0, 30, 60 and 90 days of exposition to salt-fog) are shown in

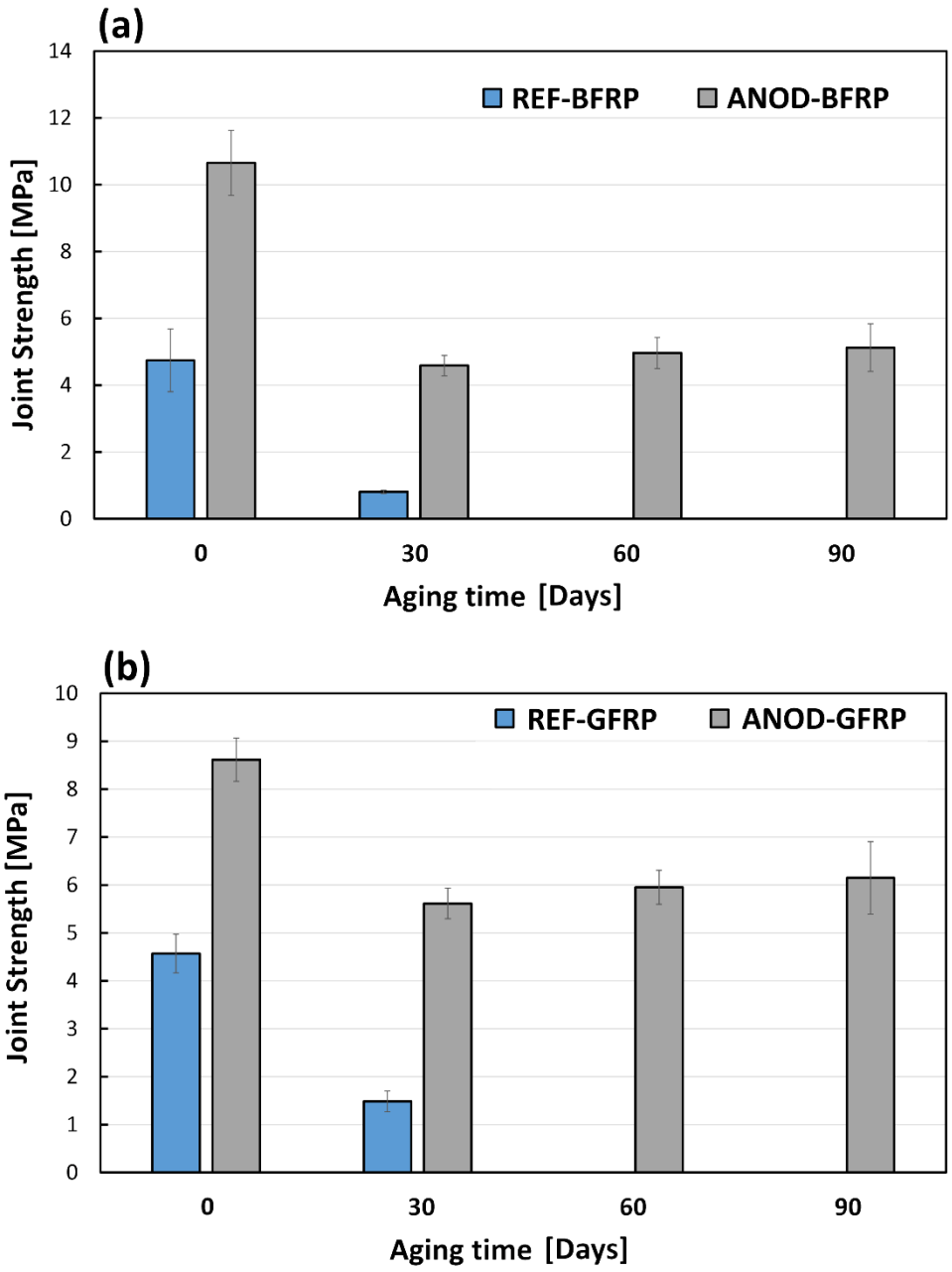

a-b.

From these figures it can be noticed that, regardless of the kind of fibres used as reinforcement of the composite substrates, REF-BFRP and REF-GFRP show dramatic reductions of their average joint strength (i.e., -83% and -67% respectively) already after 30 days of salt fog exposition.

Furthermore, it is worth noting that the strength values of these batches are missing for longer exposition times, because these samples during the cutting phase of the joints: i.e., no tensile test can be performed on REF joints (i.e., REF-BFRP and REF-GFRP) aged for 60 and 90 days. In particular, all these joint samples failed through adhesive fracture mode, evidenced by the absence of polymer matrix traces on the metal surface (Figure 4), as defined by ASTM D 5573 standard.

For the sake of brevity, only the metallic surfaces of REF-BFRP samples were shown in Figure 4, because REF-GFRP samples evidenced a quite similar behaviour, thus experiencing the same failure mode.

Moreover, Figure 4 shows the effect of humidity on the metallic surface, suggesting that water molecules were able to penetrate through the metal-composite interface. This clearly means that the exposition to the aggressive environment strongly weakens the adhesion between the mechanically abraded metal substrate and composite one, thus leading to the premature and unexpected failure of the joints during the cutting phase.

Conversely, when exposed for 30 days to the salt-fog spray condition, anodized joints (i.e., ANOD-BFRP and ANOD-GFRP) present lower decrements of their maximum strength (i.e., -57% and -35% for BFRP and GFRP, respectively) in comparison to REF joints. Consequently, ANOD joints still outperform REF joints in term of maximum strength (i.e., + 82% and + 74% for ANOD-BFRP and ANOD-GFRP) even after 30 days of aging.

Furthermore,

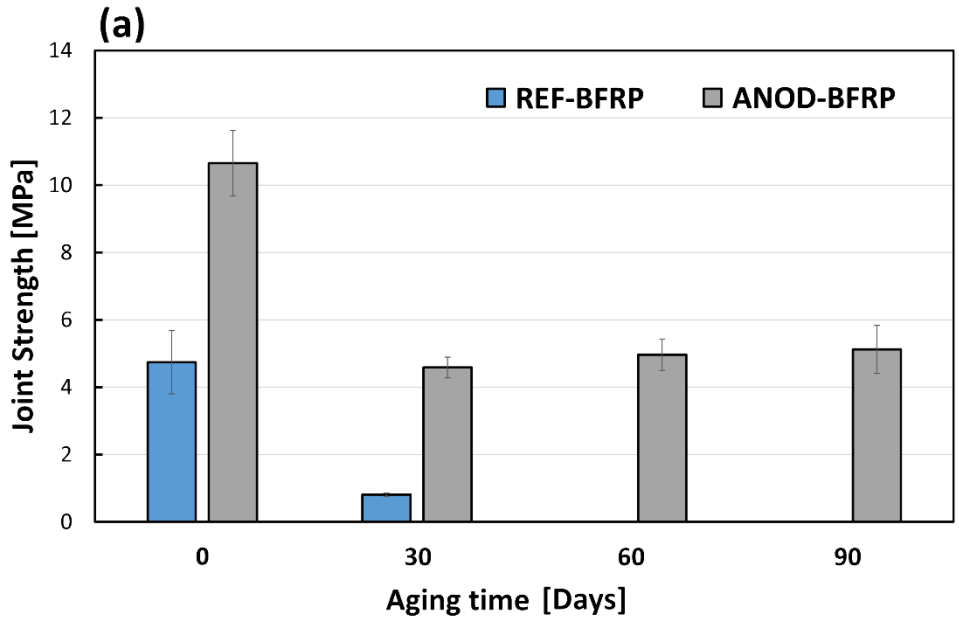

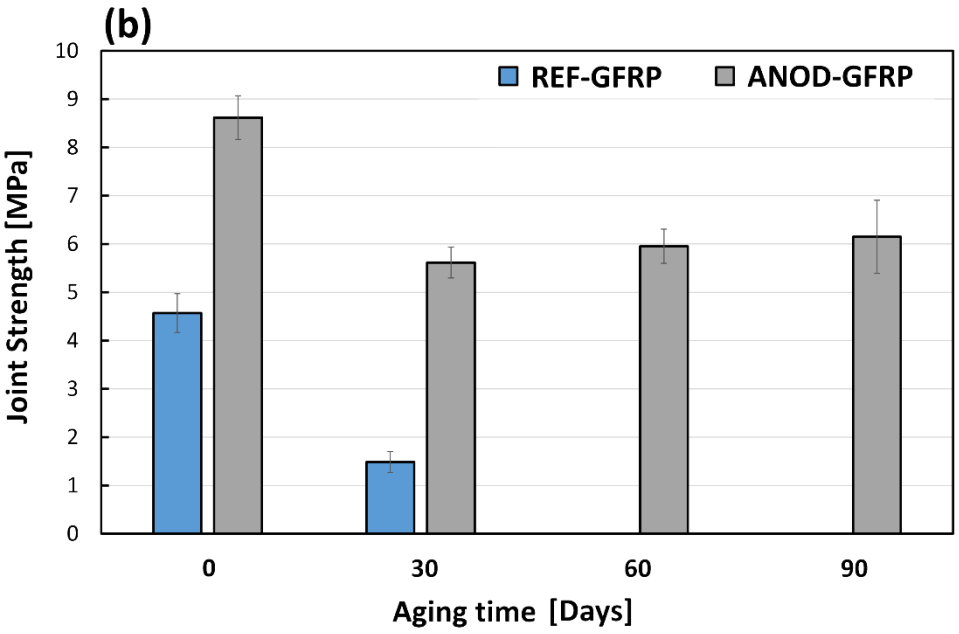

a-b clearly evidence that, regardless of kind of composite reinforcement, ANOD joints are able to keep quite constant their mechanical strength values for longer aging times. In particular, it can be noticed a slight increasing trend in the joints strength of both ANOD-GFRP and ANOD-BFRP samples for exposition time longer than 30 days.

Figure 5 shows the presence of some traces of both matrix and fiber on the metal surface of the ANOD-BFRP fractured samples, after 60 and 90 days of salt-fog exposition. This clearly means that a cohesive failure mode occurs for these joints, as defined by ASTM D 5573 standard. It is worth

noting that this failure mode occurs for all the anodized joint samples (i.e., ANOD-BFRP and ANOD-GFRP), regardless the exposition time to salt-fog.

These findings demonstrate that the anodizing process carried out by using the innovative and eco-friendly bath (i.e., TSA) allows to protect the aluminum substrate from corrosive phenomena in addition to offer a good mechanical interlocking with the epoxy matrix of the composite substrates.

By taking into account the experimental evidences from our previous work [31], the results of the present paper clearly highlight the beneficial effect of the proposed electrochemical treatment not only on the mechanical strength of bonded joints, but also on their durability when exposed to hostile environments such as marine one.

Nevertheless, it is worth stating that the strength reductions experienced by ANOD joints after the first 30 days of salt-fog exposition cannot be considered negligible (i.e., -57% and -35% for ANOD-BFRP and ANOD-GFRP samples, respectively). These results can be explained by evaluating the aging behaviour of the neat epoxy matrix. To this scope, the quasi-static flexural properties of the matrix at varying the exposition time to salt-fog are reported in Table 2. From these data, it is possible to notice that the thermoset matrix experienced noticeable decrements in the flexural strength and flexural modulus already after 30 days in the climatic chamber: i.e., -87% and -89%, respectively. Moreover, the strain at break increases by about 112% after 30 days, thus showing the occurrence of evident softening and plasticization phenomena of the epoxy matrix when exposed to salt-fog environmental conditions. For longer aging times, flexural properties do not vary markedly. In particular, flexural strength and modulus decrease of about 93% and 95%, respectively, whereas the strain at break increases of about 104%, after 90 days of aging.

These results are corroborated by the water absorption experienced by the epoxy matrix during the salt-fog exposition, as shown in Figure 6. In the early phase, there is a significant increase in the weight gain: i.e., equal to about +4% after 30 days of salt–fog exposition. For longer aging times, a progressive stabilization of the absorbed water can be evidenced, reaching increase slightly higher than 5% after 60 and 90 days.

3.2. Analysis of the failure zones

The metallic surface of the fractured joints was analysed by SEM microscope equipped with EDX analyser, to gain more insight on the fracture mechanisms of the joints.

As shown in Figure 7a-b, the metallic surface after 30 days is covered by corrosion products, mainly containing Al and O according to EDX analysis (see Figure 9). Moreover, it is possible to see that corrosion products are also present under the matrix (i.e., indicated by green arrows in Figure 7), suggesting that water is easily absorbed by the matrix and reaches the metallic substrate. As soon as water reaches the mechanically treated Al surface, extensive hydration of the native oxide produces oxyhydroxide or hydroxide phases such as AlOOH and $Al(OH)_3$ that are thermodynamically more stable than Al_2O_3 at room temperature (Figure 8). The rate of growth of oxyhydroxide and hydroxide scales is reported to proceed in three stages: 1) an induction period (of minutes to hours depending on temperature) during which no growth is observed (the native oxide does not change in thickness), 2) a period of rapid growth during which a pseudoboehmite (AlOOH) layer forms and grows to a thickness of several microns, and 3) a period of slower growth in which $Al(OH)_3$ grows on top of the pseudoboehmite. The induction period for the uniform corrosion of aluminum could correspond to the time required for a hydration front to move through the native oxide, compromising its ability to function as a diffusion barrier toward aggressive environment and inducing Al oxidation and consequent H_2 evolution. The latter process compromises the matrix adhesion.

This phenomenon is so pronounced that after 60 and 90 days of salt-fog exposition the adhesion was totally compromised. Hence, the solicitation of the rotating blade for cutting the samples led to the premature delamination of both REF-BFRP and REF-GFRP joints.

The presence of an anodic porous layer changes the phenomena occurring during aging. Figure 10 shows that the polymeric matrix with a clear footprint of fibers remains attached to the surface of the Al alloy even after 90 days of salt-fog expostion. The fracture zones are always located where fibers at 0° and 90° intertwine (i.e., indicated by red arrows in figure), disclosing the porous oxide layer of the anodized surface. For samples after 30 days of aging, the fracture zone is free of corrosion

products, suggesting that the anodic layer is stable during aging. For longer duration of the salt spray test (namely 60 days) the presence of hydration products is evident is some areas due to the hydrolysis of anodic Al_2O_3 and consequent formation of AlOOH and/or $Al(OH)_3$ (indicated by green arrows in figure), as confirmed by EDX results.

After 90 days of salt-fog-exposition, SEM micrograph at high magnification (Figure 11, yellow arrows) reveals that the anodic layer is more hydrated due to the longer exposure to the aggressive environment.

As explained above, for mechanically treated alloys (i.e., REF-BFRP and REF-GFRP) the hydration of the few nanometer thick native oxide and the subsequent Al oxidation and H_2 evolution are responsible for the drop of the joints mechanical properties already after the first month of salt-fog exposition. Conversely, for the anodized joint samples (i.e., ANOD-BFRP and ANOD-GFRP), the alloy surface is protected by few micrometer thick anodic film. Hence, the drop of the joint strength (see Figure 3) is due to the water absorption of the matrix, which leads to the weakening of the chemical bonds between the metallic substrate and the epoxy matrix [40]. The slight strength recovery for longer exposure time (i.e., 60 and 90 days, see

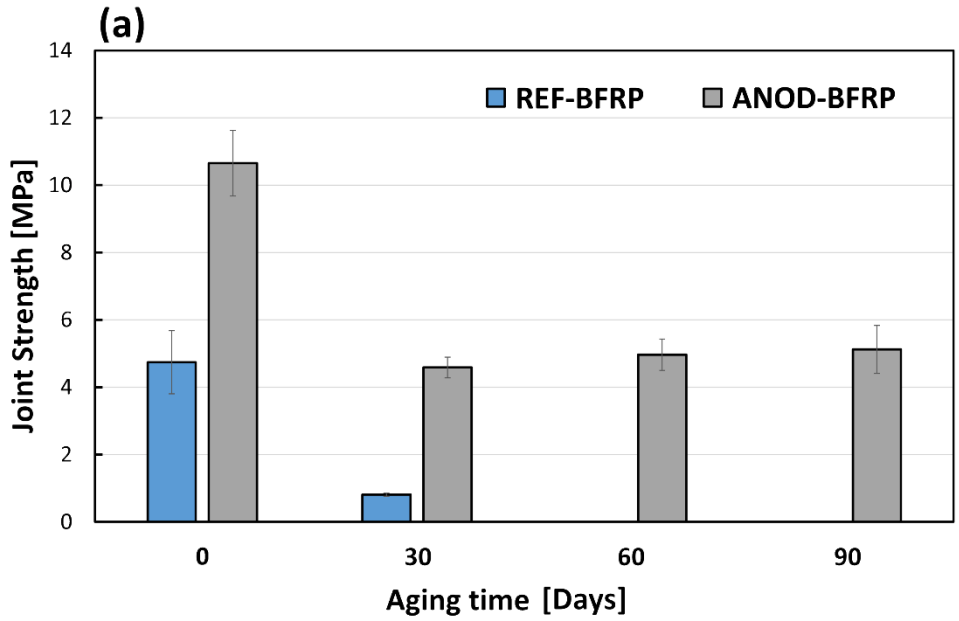

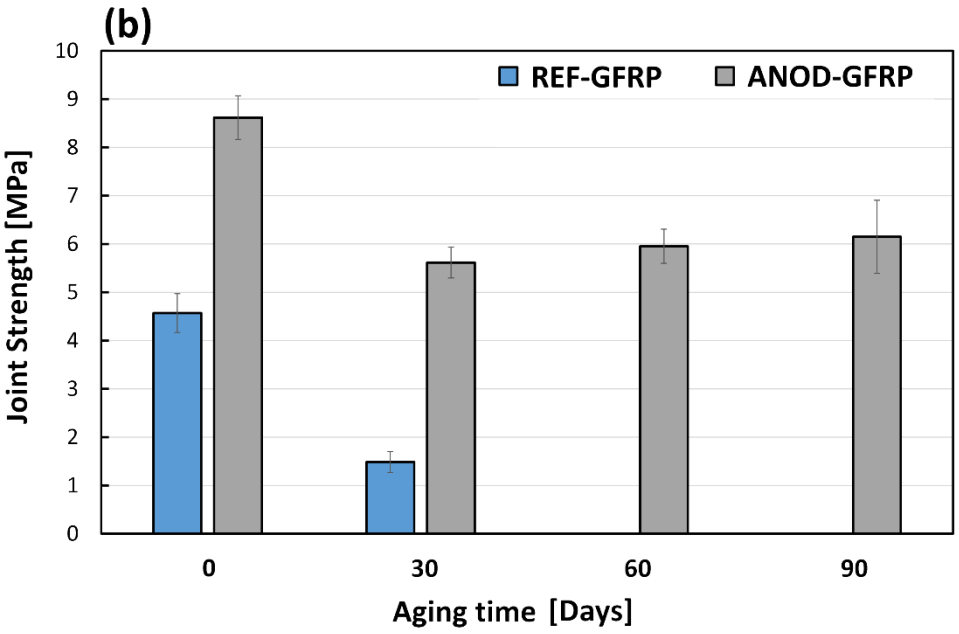

) can be explained by the improvement of the matrix adhesion with the metal alloy, due to the increased hydration degree suggested by SEM and EDX analysis. Indeed, according to the literature [40] the adhesion between the epoxy matrix and the anodized Al alloy in wet condition improves by increasing the OH^- concentration on the sample surface. According to the authors [40], the interfacial bonding proceeds through the surface hydroxyls and thus is positively influenced by the hydration. This can justify the mechanical properties recovery of ANOD joints during the salt-fog exposition.

Conclusions

Metal to composite bonded joints were prepared by performing two metal surface treatments: i.e., mechanical abrasion (REF-BFRP and REF-GFRP) and anodization with an innovative TSA bath (ANOD-BFRP and ANOD-GFRP). The evolution of the mechanical strength of these joints was monitored during their exposition to salt-fog environment for a period up to 90 days, with the aim of understanding the effect of the innovative anodizing treatment on the joints durability in marine environment.

The experimental results showed that REF joints (i.e., REF-BFRP and REF-GFRP) greatly suffer the exposition to hostile environment such as salt-fog. In particular, the 30 and 60 days-aged joints experienced premature and unexpected adhesive failures during the cutting phase, meaning that the aggressive environment exposition dramatically weakens the adhesion between the mechanically abraded metal and composite substrates. Moreover, SEM analysis confirm that this treatment was totally inadequate to the scope, because the metallic surface was covered by corrosion products already after 30 days of salt-fog exposition.

Conversely, anodized joints (i.e., ANOD-BFRP and ANOD-GFRP) show lower decrement of their mechanical performances in comparison to REF joints after 30 days of salt-fog exposition. This finding is mainly due to the scarce aging resistance of the epoxy matrix. However, it is of upmost importance to evidence that the residual strength was retained by ANOD joints during the remaining 60 days of aging. In particular, a slight recovery in the joints strength can be noticed for longer exposition time (i.e., 60 and 90 days). This result can be mainly ascribed to the increased hydration degree of the metal surface (as suggested by SEM and EDX analyses), which leads to better adhesion with the polymeric matrix.

In conclusion, this paper clearly shows the beneficial effect of the innovative and eco-friendly anodizing process on the aging resistance of metal to composite bonded joints against aggressive environmental conditions such as marine one.

Furthermore, it was shown that the main responsible of the performance loss of anodized joints is the limited durability in humid environments of the epoxy matrix. Hence, the evaluation of other thermoset polymers is proposed for future work in order to further increase the aging resistance of metal to composite bonded joints.

Acknowledgments

This work was supported by Project ‘‘THALASSA – Technology and materials for safe low consumption and low life cycle cost vessels and crafts” (PON ‘‘R&C” 2014/2020).

The authors thank CALEF consortium for suppling aluminum alloy sheets.

References

1. Rubino, F.; Nisticò, A.; Tucci, F.; Carlone, P. Marine application of fiber reinforced composites: A review. *J. Mar. Sci. Eng.* **2020**, *8*.
2. Neşer, G. Polymer based composites in marine use: History and future trends. *Procedia Eng.* **2017**, *194*, 19–24.
3. Summerscales, J. Materials selection for marine composites. In *Marine Composites*; Elsevier Ltd., 2019; pp. 3–30 ISBN 9780081022641.
4. Verma, D.; Goh, K.L. Natural fiber-reinforced polymer composites: Application in marine environments. In *Biomass, Biopolymer-Based Materials, and Bioenergy: Construction, Biomedical, and other Industrial Applications*; Elsevier Ltd, 2019; pp. 51–73 ISBN 9780081024263.
5. Ansell, M.P. Natural fibre composites in a marine environment. In *Natural Fibre Composites: Materials, Processes and Applications*; Woodhead Publishing, 2013; pp. 365–374 ISBN 9780857095244.
6. Fiore, V.; Scalici, T.; Di Bella, G.; Valenza, A. A review on basalt fibre and its composites. *Compos. Part B Eng.* 2015, *74*, 74–94.
7. Asadi, A.; Baaij, F.; Mainka, H.; Rademacher, M.; Thompson, J.; Kalaitzidou, K. Basalt fibers as a sustainable and cost-effective alternative to glass fibers in sheet molding compound (SMC). *Compos. Part B Eng.* **2017**, *123*, 210–218.
8. Kessler, E.; Gadow, R.; Straub, J. Basalt, glass and carbon fibers and their fiber reinforced polymer composites under thermal and mechanical load. *AIMS Mater. Sci.* **2016**, *3*, 1561–1576.
9. Quirino, R.L.; Monroe, K.; Fleischer, C.H.; Biswas, E.; Kessler, M.R. Thermosetting polymers from renewable sources. *Polym. Int.* 2021, *70*, 167–180.
10. Xu, P.; Li, J.; Ding, J. Chemical recycling of carbon fibre/epoxy composites in a mixed solution of peroxide hydrogen and N,N-dimethylformamide. *Compos. Sci. Technol.* **2013**, *82*, 54–59.

11. Feraboli, P.; Kawakami, H.; Wade, B.; Gasco, F.; DeOto, L.; Masini, A. Recyclability and reutilization of carbon fiber fabric/epoxy composites. *J. Compos. Mater.* **2012**, *46*, 1459–1473.
12. Wang, Y.; Cui, X.; Ge, H.; Yang, Y.; Wang, Y.; Zhang, C.; Li, J.; Deng, T.; Qin, Z.; Hou, X. Chemical Recycling of Carbon Fiber Reinforced Epoxy Resin Composites via Selective Cleavage of the Carbon-Nitrogen Bond. *ACS Sustain. Chem. Eng.* **2015**, *3*, 3332–3337.
13. Cicala, G.; Mannino, S.; La Rosa, A.D.; Banatao, D.R.; Pastine, S.J.; Kosinski, S.T.; Scarpa, F. Hybrid biobased recyclable epoxy composites for mass production. *Polym. Compos.* **2018**, *39*, E2217–E2225.
14. La Rosa, A.D.; Banatao, D.R.; Pastine, S.J.; Latteri, A.; Cicala, G. Recycling treatment of carbon fibre/epoxy composites: Materials recovery and characterization and environmental impacts through life cycle assessment. *Compos. Part B Eng.* **2016**, *104*, 17–25.
15. La Rosa, A.D.; Blanco, I.; Banatao, D.R.; Pastine, S.J.; Björklund, A.; Cicala, G. Innovative chemical process for recycling thermosets cured with recyclamines® by converting bio-epoxy composites in reusable thermoplastic-an LCA study. *Materials (Basel).* **2018**, *11*.
16. Cicala, G.; Pergolizzi, E.; Piscopo, F.; Carbone, D.; Recca, G. Hybrid composites manufactured by resin infusion with a fully recyclable bioepoxy resin. *Compos. Part B Eng.* **2018**, *132*, 69–76.
17. Cao, J.; Grenestedt, J.L. Test of a redesigned glass-fiber reinforced vinyl ester to steel joint for use between a naval GRP superstructure and a steel hull. *Compos. Struct.* **2003**, *60*, 439–445.
18. Valenza, A.; Fiore, V.; Fratini, L. Mechanical behaviour and failure modes of metal to composite adhesive joints for nautical applications. *Int. J. Adv. Manuf. Technol.* **2011**, *53*, 593–600.
19. Liu, Y.; Zhuang, W. Self-piercing riveted-bonded hybrid joining of carbon fibre reinforced polymers and aluminium alloy sheets. *Thin-Walled Struct.* **2019**, *144*, 106340.
20. Zhang, X.; He, X.; Xing, B.; Wei, W.; Lu, J. Pre-holed self-piercing riveting of carbon fibre reinforced polymer laminates and commercially pure titanium sheets. *J. Mater. Process.*

Technol. **2020**, *279*, 116550.

21. Di Bella, G.; Galtieri, G.; Pollicino, E.; Borsellino, C. Mechanical characterization of adhesive joints with dissimilar substrates for marine applications. *Int. J. Adhes. Adhes.* **2013**, *41*, 33–40.
22. Fiore, V.; Alagna, F.; Di Bella, G.; Valenza, A. On the mechanical behavior of BFRP to aluminum AA6086 mixed joints. *Compos. Part B Eng.* **2013**, *48*, 79–87.
23. Mariam, M.; Afendi, M.; Abdul Majid, M.S.; Ridzuan, M.J.M.; Gibson, A.G. Tensile and fatigue properties of single lap joints of aluminium alloy/glass fibre reinforced composites fabricated with different joining methods. *Compos. Struct.* **2018**, *200*, 647–658.
24. Fiore, V.; Alagna, F.; Galtieri, G.; Borsellino, C.; Di Bella, G.; Valenza, A. Effect of curing time on the performances of hybrid/mixed joints. *Compos. Part B Eng.* **2013**, *45*, 911–918.
25. Budhe, S.; Banea, M.D.; de Barros, S.; da Silva, L.F.M. An updated review of adhesively bonded joints in composite materials. *Int. J. Adhes. Adhes.* **2017**, *72*, 30–42.
26. Banea, M.D.; Rosioara, M.; Carbas, R.J.C.; da Silva, L.F.M. Multi-material adhesive joints for automotive industry. *Compos. Part B Eng.* **2018**, *151*, 71–77.
27. Cavezza, F.; Boehm, M.; Terryn, H.; Hauffman, T. A review on adhesively bonded aluminium joints in the automotive industry. *Metals (Basel).* **2020**, *10*, 1–32.
28. Park, S.Y.; Choi, W.J.; Choi, H.S.; Kwon, H.; Kim, S.H. Recent trends in surface treatment technologies for airframe adhesive bonding processing: A review (1995-2008). *J. Adhes.* **2010**, *86*, 192–221.
29. Marques, A.C.; Mocanu, A.; Tomić, N.Z.; Balos, S.; Stammen, E.; Lundevall, A.; Abrahami, S.T.; Günther, R.; de Kok, J.M.M.; de Freitas, S.T. Review on adhesives and surface treatments for structural applications: Recent developments on sustainability and implementation for metal and composite substrates. *Materials (Basel).* **2020**, *13*, 1–43.
30. Di Franco, F.; Zaffora, A.; Santamaria, M.; Di Quarto, F. Anodization and anodic oxides. In *Encyclopedia of Interfacial Chemistry: Surface Science and Electrochemistry*; Elsevier Inc., 2018; pp. 26–40 ISBN 9780128098943.

31. Fiore, V.; Di Franco, F.; Miranda, R.; Santamaria, M.; Badagliacco, D.; Valenza, A. Effects of anodizing surface treatment on the mechanical strength of aluminum alloy 5083 to fibre reinforced composites adhesive joints. *Int. J. Adhes. Adhes.* **2021**, *108*, 102868.

32. Mohamad, M.; Marzuki, H.F.A.; Bakar, S.N.A.; Abdullah, A.N.; Ubaidillah, E.A.E.; Abidin, M.F.Z.; Omar, S. Effect of anodizing electrolyte for structural adhesives bonding study of aluminium-carbon laminates composites. *Int. J. Automot. Mech. Eng.* **2014**, *10*, 2091–2101.

33. Correia, S.; Anes, V.; Reis, L. Effect of surface treatment on adhesively bonded aluminium-aluminium joints regarding aeronautical structures. *Eng. Fail. Anal.* **2018**, *84*, 34–45.

34. Li, Y.D.; Zhao, P.Z.; Feng, Y.J.; Cao, H.L. Influence of anodic oxide film structure on adhesive bonding performance of 5754 aluminum alloy. *Trans. Nonferrous Met. Soc. China* **2019**, *29*, 1836–1841.

35. Bjørgum, A.; Lapique, F.; Walmsley, J.; Redford, K. Anodising as pre-treatment for structural bonding. *Int. J. Adhes. Adhes.* **2003**, *23*, 401–412.

36. Machalická, K. V.; Vokáč, M.; Pokorný, P.; Pavlíková, M. Effect of various artificial ageing procedures on adhesive joints for civil engineering applications. *Int. J. Adhes. Adhes.* **2020**, *97*, 102476.

37. Abdel-Monsef, S.; Renart, J.; Carreras, L.; Maimí, P.; Turon, A. Effect of environmental conditioning on pure mode I fracture behaviour of adhesively bonded joints. *Theor. Appl. Fract. Mech.* **2020**, *110*, 102826.

38. Chen, Y.; Li, M.; Yang, X.; Wei, K. Durability and mechanical behavior of CFRP/Al structural joints in accelerated cyclic corrosion environments. *Int. J. Adhes. Adhes.* **2020**, *102*, 102695.

39. Golaz, B.; Michaud, V.; Lavanchy, S.; Månson, J.A.E. Design and durability of titanium adhesive joints for marine applications. *Int. J. Adhes. Adhes.* **2013**, *45*, 150–157.

40. Abrahami, S.T.; Hauffman, T.; De Kok, J.M.M.; Mol, J.M.C.; Terryn, H. Effect of Anodic Aluminum Oxide Chemistry on Adhesive Bonding of Epoxy. *J. Phys. Chem. C* **2016**, *120*, 19670–19677.

41. Zhang, J.-S.; Zhao, X.-H.; Zuo, Y.; Xiong, J.-P. The bonding strength and corrosion resistance of aluminum alloy by anodizing treatment in a phosphoric acid modified boric acid/sulfuric acid bath. *Surf. Coatings Technol.* **2008**, *202*, 3149–3156.

42. Curioni, M.; Skeldon, P.; Koroleva, E.; Thompson, G.E.; Ferguson, J. Role of Tartaric Acid on the Anodizing and Corrosion Behavior of AA 2024 T3 Aluminum Alloy. *J. Electrochem. Soc.* **2009**, *156*, C147.

Table 1. List of manufactured joints.

Code	Metal substrate treatment	Composite substrate reinforcement
REF-GFRP	Mechanical abrasion	Glass
REF-BFRP	Mechanical abrasion	Basalt
ANOD-GFRP	Anodizing	Glass
ANOD-BFRP	Anodizing	Basalt

Table 2. Three-point bending properties of neat matrix at varying the exposition time to salt-fog.

Aging time [days]	**Flexural strength [MPa]**	**Variation [%]**	**Flexural Modulus [GPa]**	**Variation [%]**	**Strain at break [%]**	**Variation [%]**
0	78.6 ± 10.1		2.6 ± 0.2		3.5 ± 0.7	
30	10.5 ± 0.8	-86.6%	0.3 ± 0.03	-89.2%	7.5 ± 0.8	+112.6%
60	5.8 ± 0.2	-92.6%	0.14 ± 0.05	-94.6%	7.3 ± 0.4	+106.3%
90	5.1 ± 0.5	-93.5%	0.13 ± 0.03	-94.9%	7.2 ± 0.5	+103.9%

Table captions

Table 1. List of manufactured joints.

Table 2. Quasi-static three-point bending results of the neat matrix at varying the exposition time to salt-fog.

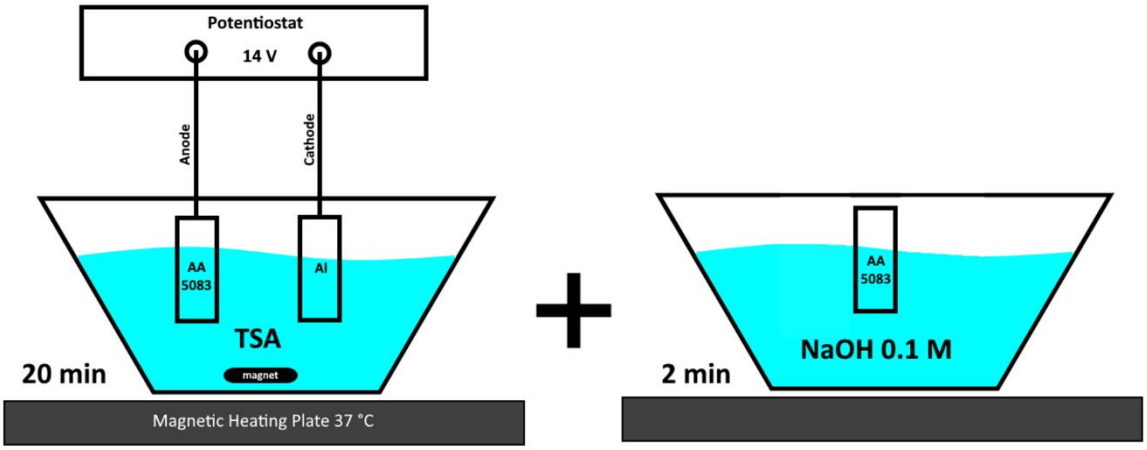

Figure 1. Schematic representation of electrochemical treatment on aluminum alloy surface.

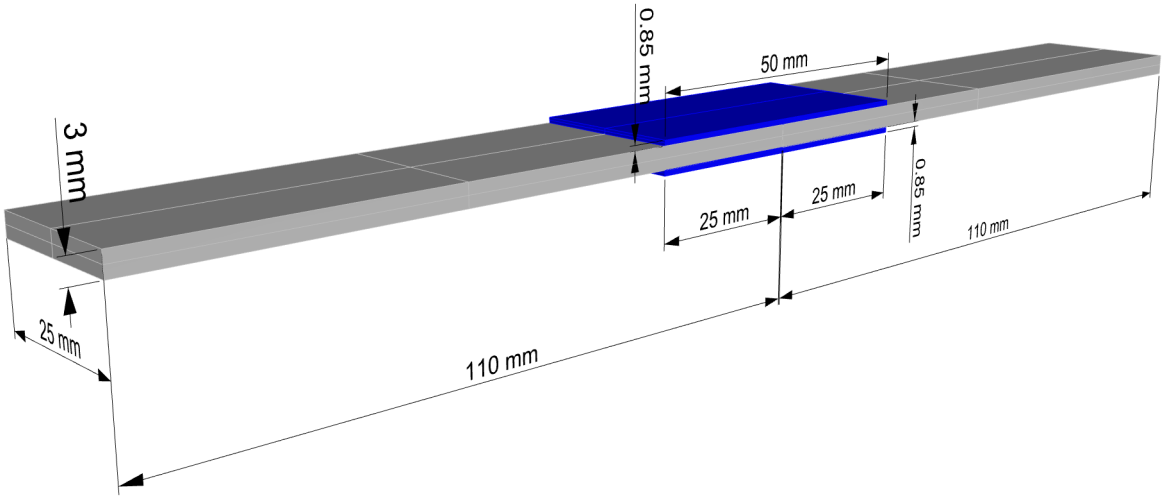

Figure 2. Schematization of joint sample – Gray: AA 5083; Blue: Composite substrate.

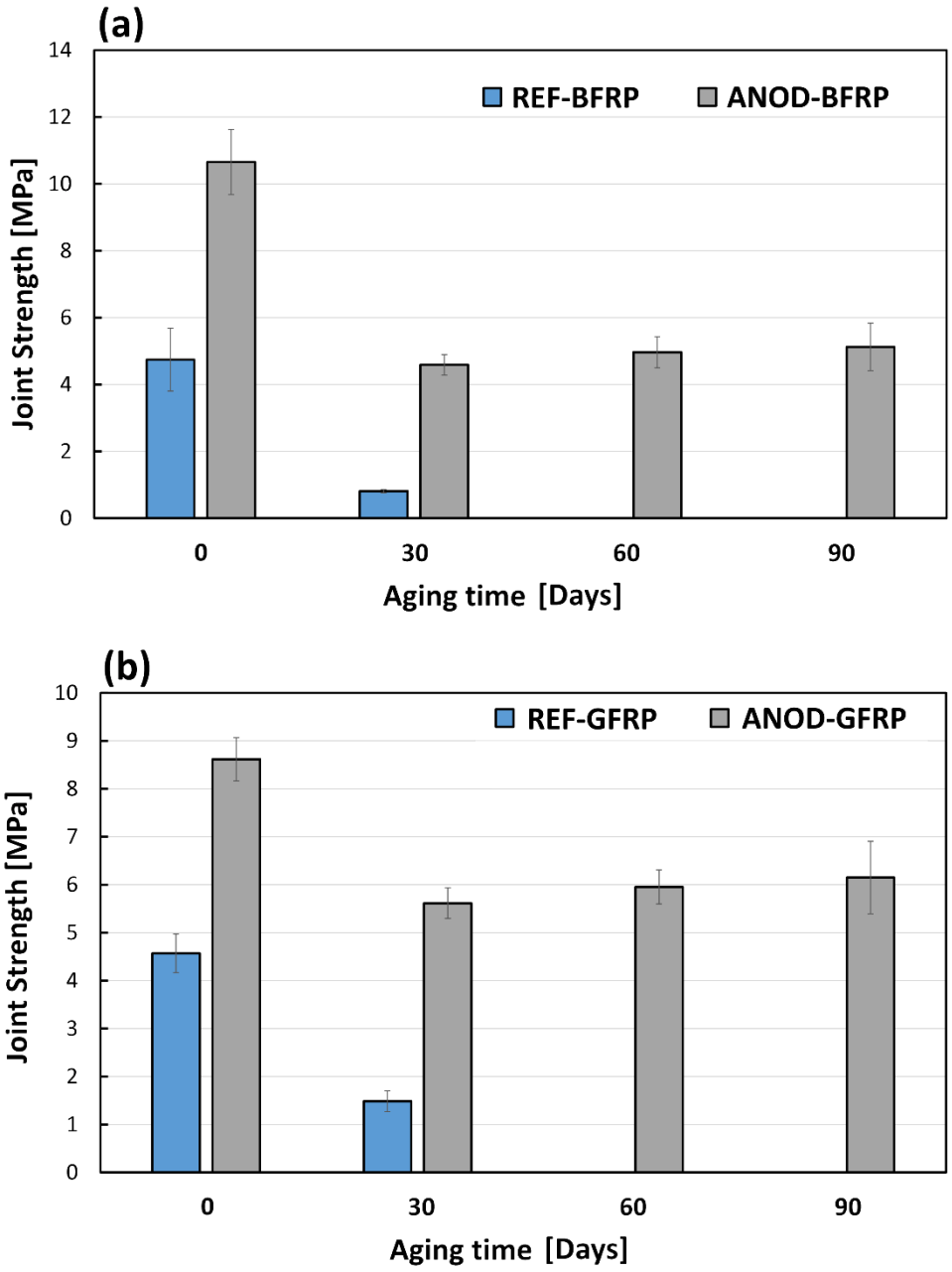

Figure 3. Strength average values versus aging time of joints with a) basalt and b) glass fibers as reinforcement of composite substrates.

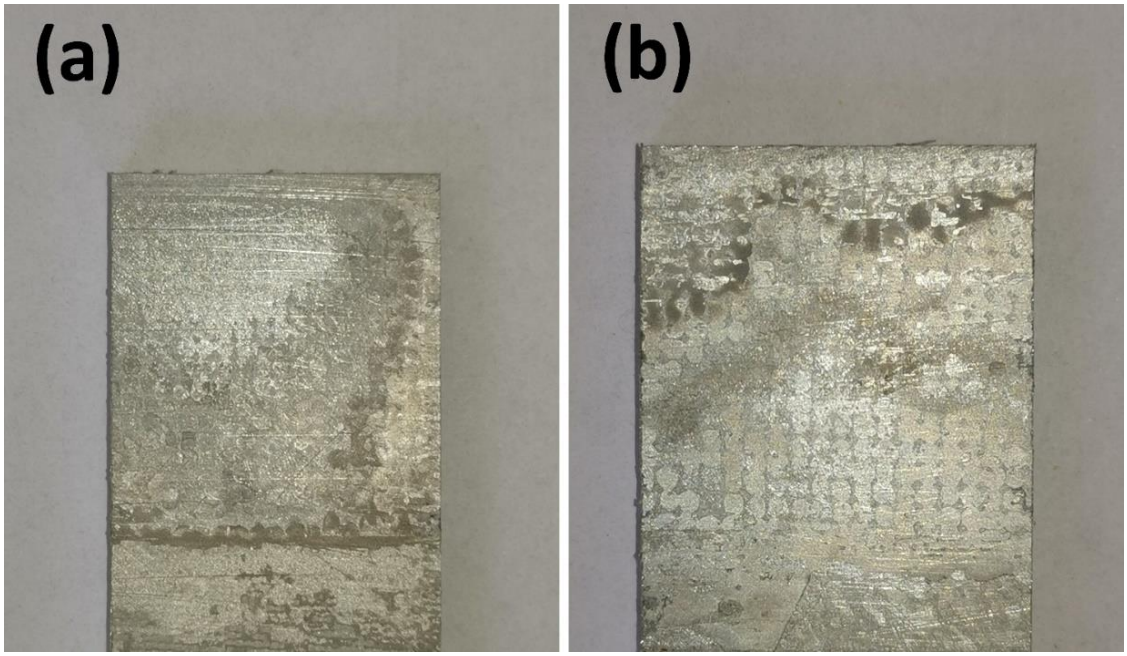

Figure 4. Aluminum alloy surfaces of REF-BFRP joint samples exposed to salt-fog for (a) 60 days and (b) 90 days.

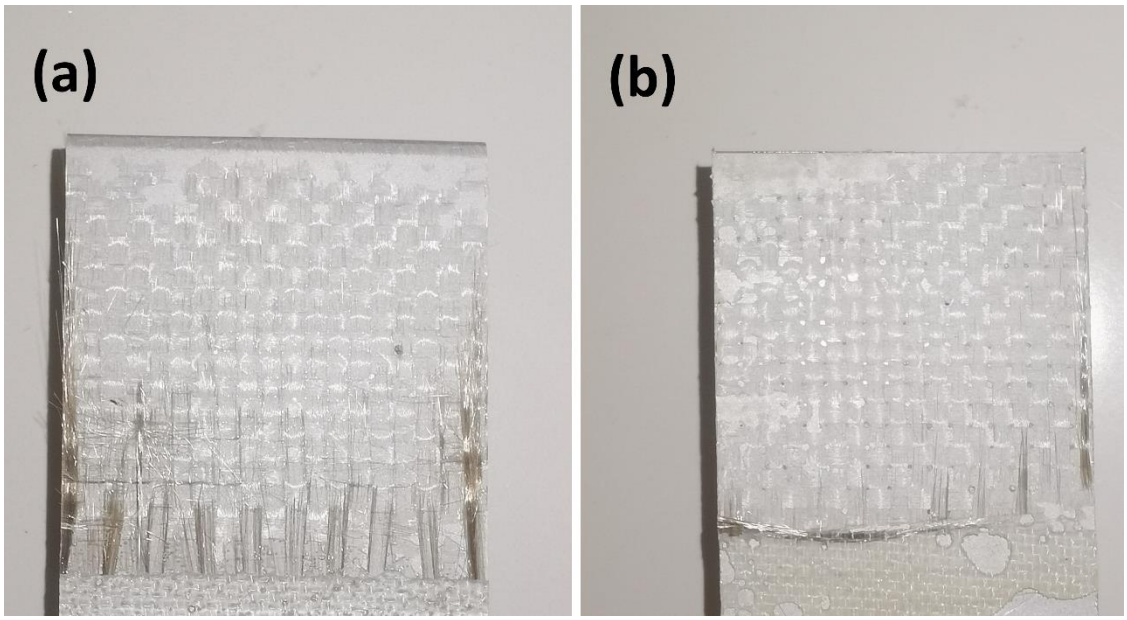

Figure 5. Aluminum alloy surfaces of ANOD-BFRP joint samples exposed to salt-fog for (a) 60 days and (b) 90 days.

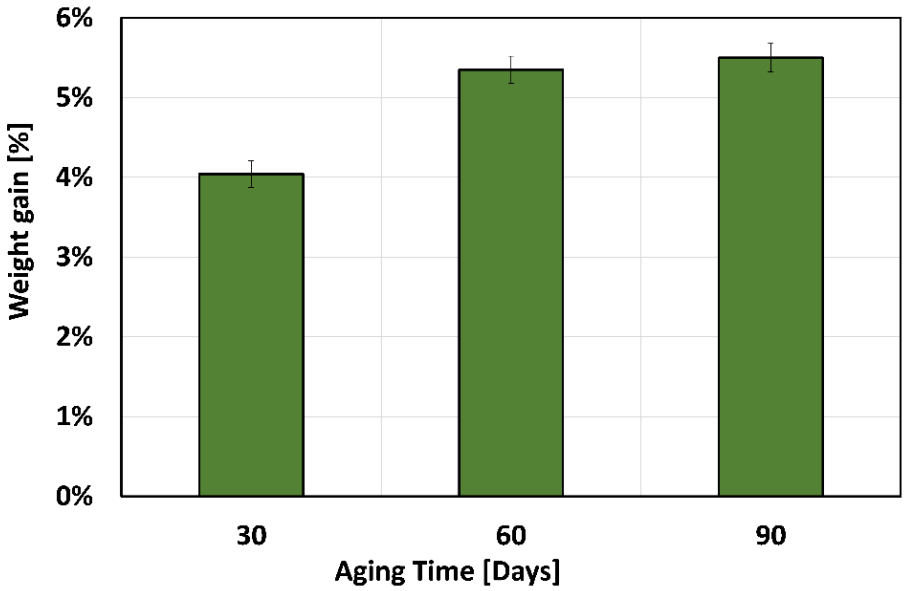

Figure 6. Weight gain of neat matrix at varying the exposition time to salt-fog**.**

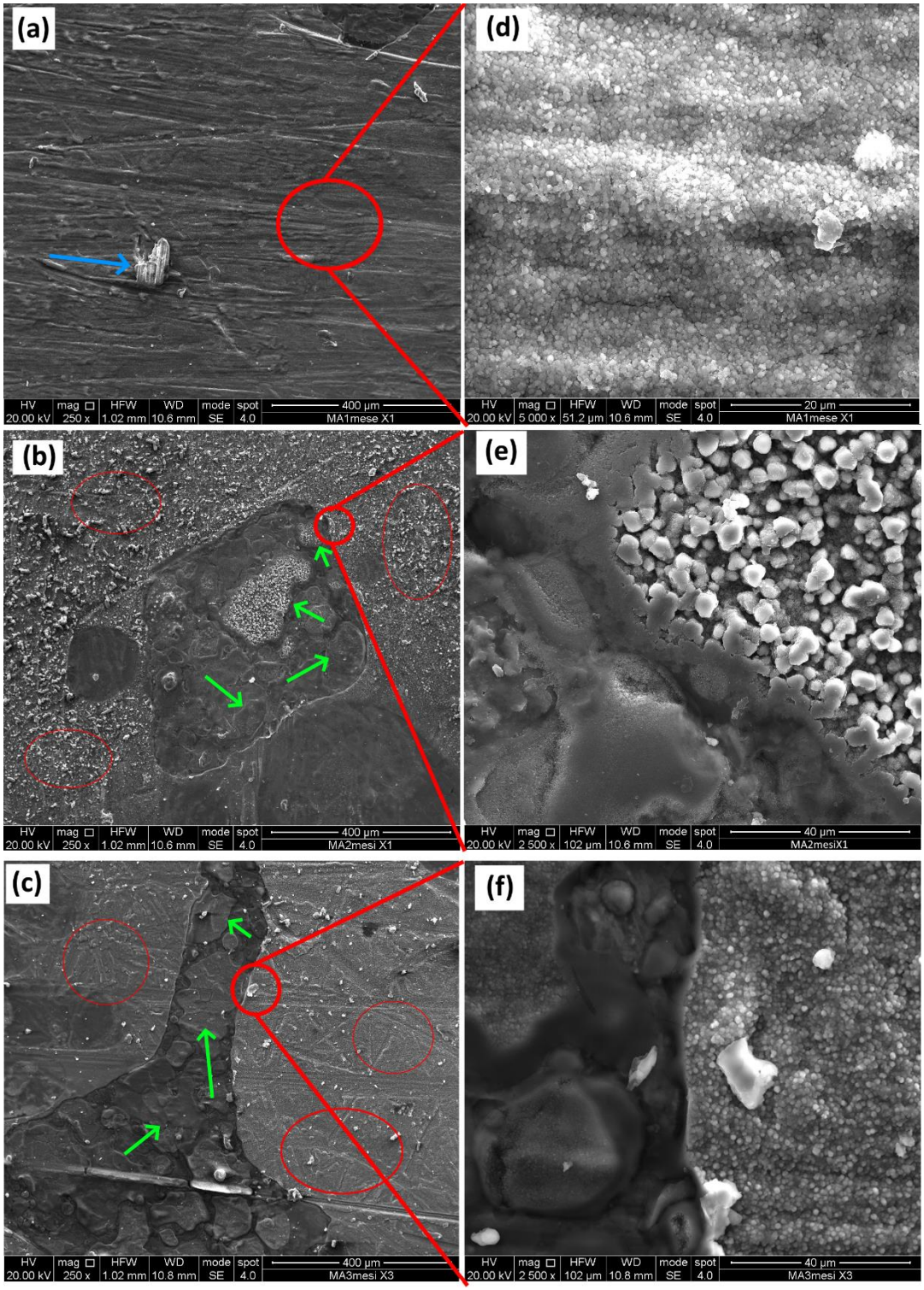

Figure 7. SEM micrographs of the metal surface of fractured REF-BFRP joint samples after a-d) 30 days, b-e) 60 days and c-f) 90 days of salt-fog exposition.

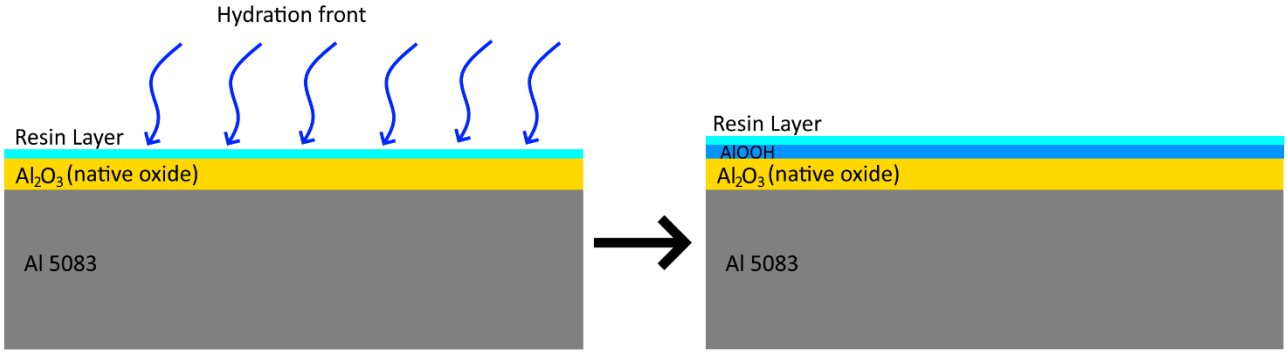

Figure 8. Schematization of uniform corrosion on the mechanical treated aluminum surface exposed to salt-fog spray conditions.

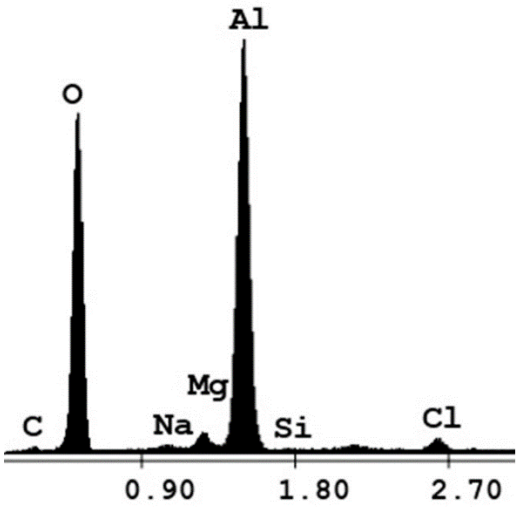

EDAX ZAF Quantification
Element Normalized
SEC Table : Default

Element	Wt %	At %
C	4.78	7.50
O	54.41	64.06
Na	0.59	0.48
Mg	1.69	1.31
Al	36.93	25.78
Si	0.15	0.10
Cl	1.45	0.77
Total	100.00	100.00

Figure 9. EDX analysis of the metal fracture surface of REF-BFRP after 30 days of salt-fog exposition.

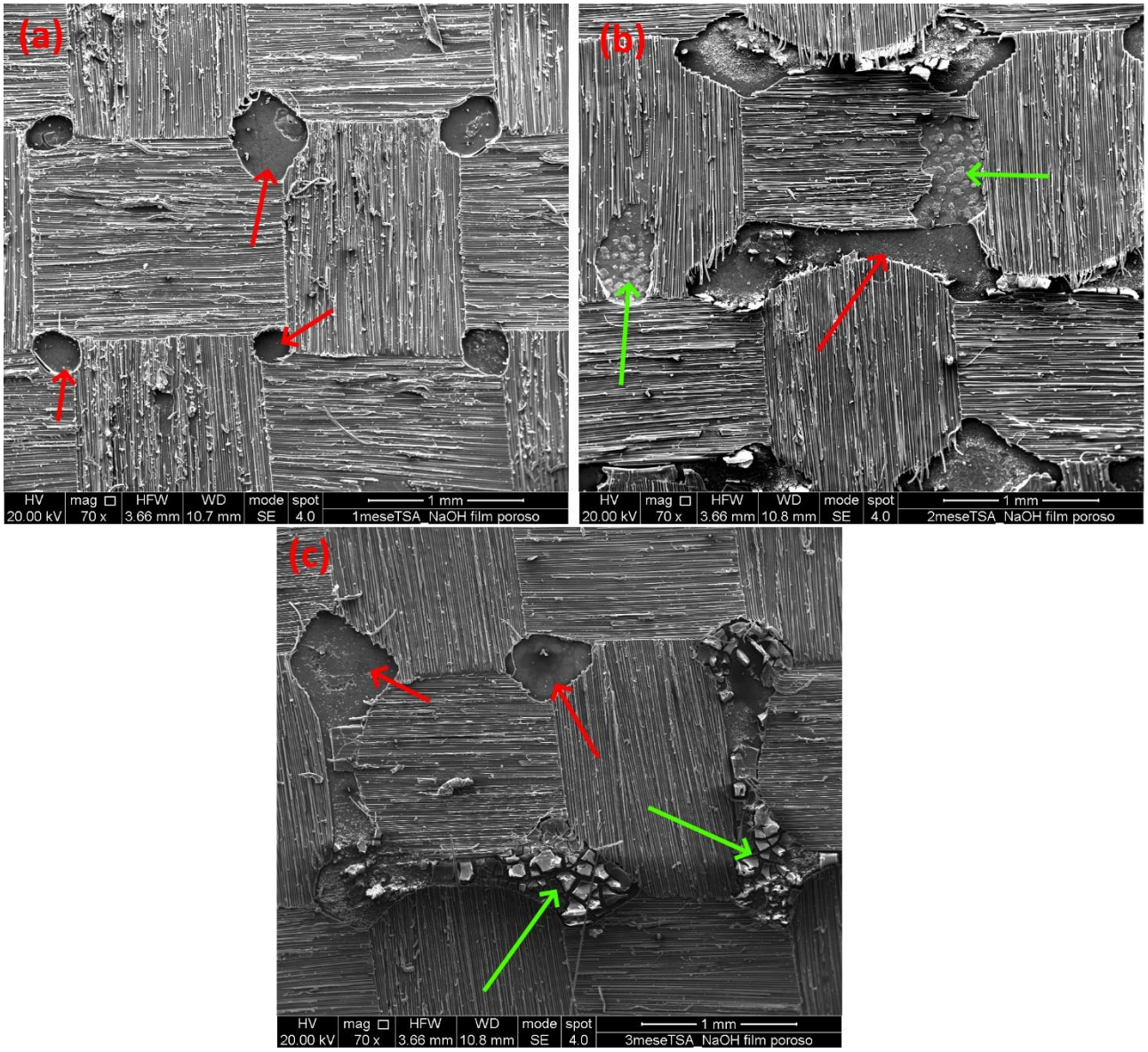

Figure 10. SEM micrographs at low magnification of the metallic surface of fractured ANOD-BFRP joint samples after a) 30 days, b) 60 days and c) 90 days of salt-fog exposition.

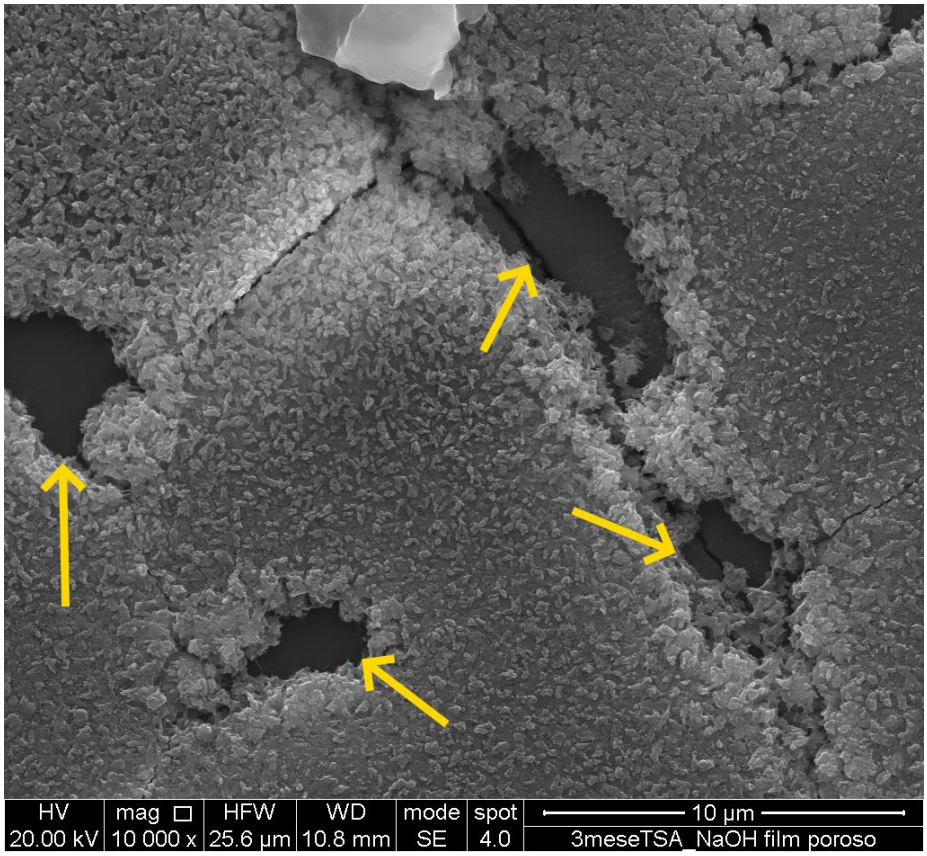

Figure 11: SEM micrograph at high magnification of the anodic layer on the metallic surface of ANOD-BFRP joint sample after 90 days of salt-fog exposition.

Figure captions

Figure 1. Schematic representation of electrochemical treatment on aluminum alloy surface.

Figure 2. Schematization of joint sample – Gray: AA 5083; Blue: Composite substrate.

Figure 3. Strength average values versus aging time of joints with a) basalt and b) glass fibers as reinforcement of composite substrates

Figure 4. Aluminum alloy surfaces of REF-BFRP joint samples exposed to salt-fog for (a) 60 days and (b) 90 days.

Figure 5. Aluminum alloy surfaces of ANOD-BFRP joint samples exposed to salt-fog for (a) 60 days and (b) 90 days.

Figure 6. Weight gain of neat matrix .

Figure 7. SEM micrographs of the metal surface of fractured REF-BFRP joint samples after a-d) 30 days, b-e) 60 days and c-f) 90 days of salt-fog exposition.

Figure 8. Schematization of uniform corrosion on the mechanical treated aluminum surface exposed to salt-fog spray conditions.

Figure 9. EDX analysis of the metal fracture surface of REF-BFRP after 30 days of salt-fog exposition.

Figure 10. SEM micrographs at low magnification of the metallic surface of fractured ANOD-BFRP joint samples after a) 30 days, b) 60 days and c) 90 days of salt-fog exposition.

Figure 11: SEM micrograph at high magnification of the anodic layer on the metallic surface of ANOD-BFRP joint sample after 90 days of salt-fog exposition.